Theoretical study of CH 4 photodissociation on Pd and Ni(111) surfaces

Yoshinobu Akinaga, Tetsuya Taketsugu, and Kimihiko Hirao

Citation: The Journal of Chemical Physics **109**, 11010 (1998); doi: 10.1063/1.477739
View online: http://dx.doi.org/10.1063/1.477739
View Table of Contents: http://scitation.aip.org/content/aip/journal/jcp/109/24?ver=pdfcov
Published by the AIP Publishing

Theoretical study of CH_4 photodissociation on Pd and Ni(111) surfaces

Yoshinobu Akinaga, Tetsuya Taketsugu, and Kimihiko Hirao
Department of Applied Chemistry, Graduate School of Engineering, The University of Tokyo, Tokyo 113, Japan

(Received 28 July 1998; accepted 21 September 1998)

Photofragmentations of a methane molecule adsorbed on Pd and Ni(111) surfaces have been studied by means of density functional theory (DFT) and *ab initio* molecular orbital calculations. The metal surfaces were represented approximately by finite metal clusters M_n ($n=1$, 7, 10). The CH_4-3s Rydberg excited state is found to be stabilized by about 2.0 and 1.5 eV through the physisorption on Pd and Ni metal surfaces, respectively. This stabilization can be understood as the results of the electron transfer from adsorbates to metal surfaces through an overlap between the CH_4 Rydberg orbital and the metal *s* orbital. Potential energies of the ground and several excited states for the $H_3C\cdots HM_n$ system as functions of the C···H distance suggest that the charge transfer states lead to the fragmentation of CH_4 to CH_3 and H. The CH_4 photodissociation for Pd and Ni(111) surfaces occurs through a direct excitation and the mechanism is basically the same as what we found for the CH_4/Pt(111) system [J. Chem. Phys. **107**, 415 (1997)]. © *1998 American Institute of Physics.* [S0021-9606(98)31148-4]

I. INTRODUCTION

The photodissociation of CH_4 has been studied both experimentally[1,2] and theoretically.[3,4] According to the experimental result,[1,2] CH_4 shows continuous absorption spectra beginning from 145 nm (8.6 eV photon) due to a predissociation, and the first-excited triply degenerate state 1^1T_2 (Rydberg type) lies about 10 eV above the ground state, which is crossed by a valence antibonding state leading to the dissociation. Absorption peaks at 9.7 and 10.3 eV originate from this excited state, of which degeneracy has been broken through the Jahn–Teller effect.[1] Recently, Matsumoto *et al.* studied photodissociations of CH_4 on Pt and Pd(111) surfaces experimentally,[5] and detected several points as follows: the CH_4 molecule physisorbs on Pt and Pd(111) surfaces with the adsorption energy of about 5 kcal/mol [the adsorption energy on Pt(111) is slightly smaller than that on Pd(111)]: a thermal desorption was observed at 70 K. On the other hand, with an irradiation of a pulse laser with the wavelength of 193 nm, the thermal desorption was observed not only at 70 K but also at 250 K. This desorption of CH_4 at 250 K should be the result of the photodissociation of CH_4 by the 6.4 eV photon; the CH_4 desorbed at 250 K may be created through a recombination of CH_3 and H species adsorbed on the surface, which are the products of the dissociation of CH_4 invoked by the photon irradiation.

Generally, there are two distinguishable mechanisms for the photon absorption by the adsorbate–substrate system:[6] a direct excitation in which the photon absorption is localized on the adsorbate, and a surface-mediated electron attachment in which a hot electron created via photon absorption on the surface is transferred to the adsorbate to form a transient negative ion state which undergoes the reaction. The direct excitation is observed on the dielectric or semiconductor surface with large band gaps, while the surface-mediated mechanism is often applied to transition metal surfaces. As to the photodissociation of CH_4 on the Pt and Pd(111) surfaces, Matsumoto *et al.* measured the polarization-dependent photochemical cross section as a function of the incident angle,[5] and concluded that the direct excitation of CH_4 plays an essential role. Since CH_4 shows absorption spectra in the region <145 nm (above 8.6 eV photon), the direct excitation of adsorbed CH_4 on the surface by the 193 nm (6.4 eV photon) indicates that the excited state of CH_4 is stabilized through the interaction with the metal surface by ~ 2 eV. Such a strong interaction is rather remarkable, since it would be expected that the electronic structure of CH_4 is not largely perturbed by the adsorption because of the physisorption (the adsorption energy is small). So, the mechanism for the stabilization of the Rydberg excited state of CH_4 through the adsorption has been unidentified.

Very recently, we carried out *ab initio* molecular orbital calculations to clarify the mechanism of the photodissociation of CH_4 adsorbed on the Pt(111) surface using a finite cluster approximation, and found that the Rydberg excited state of CH_4 is largely stabilized through the interaction with the Pt(111) surface, in which the electron transfer is invoked from the CH_4 3*s*-Rydberg orbital to the Pt 6*s* orbital because of their large spatial extents.[7] This stabilization explains well the shift of the absorption wavelength observed in the experiment. We also calculated potential energy curves (PECs) of ground and several excited states for $H_3C\cdots H{-}Pt_n$ ($n=1,4$) as a function of the distance of C···H, showing that the transition to the charge transfer state leads to the dissociation of CH_3 and $H{-}Pt_n$.[7]

In present work, we apply the same calculations to the photodissociation of CH_4 on Pd and Ni(111) surfaces, to verify the similarity and the difference from the reaction mechanism detected for the CH_4/Pt(111) system. A fragmentation of CH_4 using a nickel catalyst is an industrially important reaction. and has been extensibly studied both experimentally[8–13] and theoretically,[14,15] but most of those

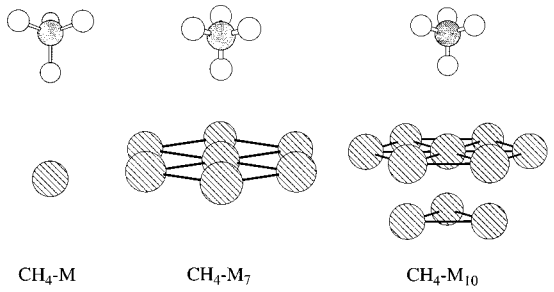

FIG. 1. Adsorption structures CH_4–M_n (M=Pd, Ni; $n=1$, 7, 10).

TABLE I. Geometrical parameters[a] and adsorption energies E_{ads} (kcal/mol) determined by the B3LYP method for CH_4 and CH_4–M_n (M=Pt, Pd, Ni; $n=7$, 10).

	$r(H_{ad}–M)$	$r(C–H_{ad})$	$r(C–H)$	$a(HCH_{ad})$	E_{ads}
CH_4	···	1.100	1.100	109.47	···
CH_4–Pt_7	3.000	1.100	1.100	109.44	0.67
CH_4–Pt_{10}	2.437	1.104	1.097	109.26	0.91
CH_4–Pd_{10}	2.254	1.104	1.097	109.40	2.35
CH_4–Ni_{10}	2.365	1.103	1.097	109.33	3.63

[a]Bond length r in Å: bond angle a in deg.

studies have been concerned mainly with the thermal reactions. In our calculations, the attention should be paid to photoreactions of CH_4 on the Ni(111) surface.

II. COMPUTATIONAL DETAIL

The computational methods are basically the same as those employed for the CH_4/Pt(111) system.[7] The Pd and Ni(111) surfaces were represented by bare metal clusters M_n ($n=1$, 7, 10) as shown in Fig. 1. The CH_4 molecule interacts with Pd and Ni(111) surfaces weakly as with the Pt(111) surface, so it is necessary to use a large metal cluster to determine the adsorption structure because small clusters cannot mimic the weak interaction, probably due to the insufficient representation of the exchange repulsion between an approaching molecule and the surface.[7] So, the adsorption structure of CH_4 was determined for CH_4–M_{10} (M=Pd, Ni) by the density functional theory (DFT)-based method, B3LYP with Becke's three-parameter functional using the Lee–Yang–Parr nonlocal correlation functional.[16–18] As shown in Fig. 1, CH_4 was assumed to approach an on-top site of the metal surface with one hydrogen atom pointed to the surface. The advantage of such an adsorption structure was verified for the Pt(111) surface through comparisons with other adsorption sites or molecular orientations.[7]

Calculations of excited states for the $H_3CH\cdots M_n$ system were carried out by means of the state-averaged complete active space self-consistent field (SA-CASSCF) method,[19] in which eight valence and $3s$-Rydberg orbitals of CH_4, one d orbital having a large overlap with CH_4 orbitals [as near as possible to the metal highest occupied molecular orbital (HOMO)], and one unoccupied s orbital of the metal cluster were taken as active orbitals basically, that is, ten electrons in eleven orbitals [which is referred to as (10/11)]. The remaining occupied orbitals were treated as frozen core orbitals. The reference orbitals for SA-CASSCF calculations were obtained by restricted Hartree–Fock (RHF) calculations for the CH_4–M_n system, or other techniques which will be described later.

For C and H, Dunning's augmented cc-pVDZ basis sets[20] were used. For Pd (or Ni), the Kr (or Ar) core was replaced by the effective core polentials while valence $nd(n+1)s(n+1)p$ electrons were treated explicitly by $(3s3p4d)/[2s2p2d]$ (or $(3s2p5d)/[2s2p2d]$) Gaussian basis functions.[21] For calculations with the cluster of ten metal atoms, valence basis sets for metal atoms except the adsorbed atom M_{ad} were reduced to $[2s1p1d]$. Geometry optimizations and calculations of the excited states were carried out using the GAUSSIAN94[22] and the MOLPRO96[23] programs, respectively.

III. RESULTS AND DISCUSSION

A. Adsorption structure

A methane molecule is known to physisorb on Pt, Pd, and Ni(111) surfaces.[5,24] Geometrical parameters and adsorption energies of CH_4 on Pt_7, Pt_{10}, Pd_{10}, and Ni_{10} clusters determined by the B3LYP method are given in Table I. It is seen that the ten-atom cluster (Pt_{10}) gives a shorter surface–molecule distance and a larger adsorption energy than the seven-atom cluster (Pt_7). Because of the presence of the second layer atoms, the electron cloud of the ten-atom cluster can polarize to reduce the exchange repulsion with CH_4, but not to such an extent as the four-atom cluster, in which the adsorption energy was overestimated as about 10 kcal/mol.[7]

A molecular desorption of CH_4 on the Ni(111) surface is observed at a lower temperature than on Pt or Pd(111) in the experiments, so the order of the adsorption energy of CH_4 on metal surfaces may be Ni<Pt<Pd.[24] For ten-atom clusters, however, the order of the calculated adsorption energy among three metal surfaces is Pt<Pd<Ni. Note that it is difficult to estimate such small differences in the physisorption energy as a few kcal/mol or less by the calculation using a finite cluster approximation for transition metal surfaces. In the following, we employed the adsorption structures given in Table I to the study of the CH_4 photodissociation on metal surfaces.

B. Pd(111) surface

1. CH_4–Pd

We calculated the electronic structures of ground and excited states of CH_4–Pd by means of the SA-CASSCF method with the (10/11) active space. One metal atom is, of course, too simple to represent the metal surface, but we expect it can give the physical insight related to the surface reaction, as in the Pt(111) case.[7] Geometrical parameters as the H–Pd distance and CH_4 molecular structures were fixed to optimized values determined for the CH_4–Pd_{10} system given in Table I. Pd has an electronic configuration of $4d^{10}$ (^1S) in the ground state. In CH_4–Pd, the electronic configuration of Pd does not vary largely, i.e., $d^{9.9}s^{0.0}$, since

TABLE II. Leading configurations,[a] the excitation energy (eV), and the oscillator strength (a.u.) for ground and excited states of CH_4–Pd_7 calculated by the SA-CASSCF (10/12) method.

State[b]	Natural orbitals[c]				Coefficient	Excitation energy	Oscillator strength
	CH–a_1	$4d_{z^2}$	$5s-\sigma$	$5s-\sigma^*$			
X^1A_1	2	2	0	0	0.960	···	···
2^1A_1	2	1	1	0	0.941	1.80	1.104×10^{-3}
3^1A_1	2	1	0	1	−0.775	5.30	4.015×10^{-2}
	2	0	2	0	0.581		
4^1A_1	2	1	0	1	0.560	5.61	2.723×10^{-2}
	2	0	2	0	0.720		
5^1A_1	1	2	1	0	0.854	8.98	1.588×10^{-1}
	1	1	2	0	−0.381		

[a]With an absolute value larger than 0.3.
[b]2^1A_1, 3^1A_1, and 4^1A_1 correspond to the intracluster excited states; 5^1A_1 corresponds to the lowest charge transfer state.
[c]$4d_{z^2}$ denotes Pd_7–$4d_{z^2}$ orbitals; $5s-\sigma$ denotes the bonding orbital between Pd_7–$5s$ and CH_4–$3s$; $5s-\sigma^*$ denotes the corresponding antibonding orbital.

the interaction between CH_4 and Pd is weak in the ground state (the interaction energy was calculated as 1.13 kcal/mol).

In the previous study for a CH_4/Pt system,[7] we found that the Rydberg state of CH_4 interacts with the Pt atom through the electron donation from the CH_4 $3s$-Rydberg orbital to the Pt $6s$ orbital to form a charge transfer state with the excitation energy of 8.36 eV, leading to the dissociation of CH_{ad} H_{ad} denotes the hydrogen atom in the side of the metal atom).[7] Note that the excitation energy of 1^1T_2 state of the isolated CH_4 is calculated as 10.16 eV. For the CH_4–Pd system, it is also found that the similar charge transfer state appears with the excitation energy of 9.34 eV. This difference in the excitation energy between CH_4–Pt and CH_4–Pd may be due to the difference of a metal s orbital energy. This point will be discussed later. We also calculated PECs of ground and excited states of CH_4–Pd with respect to the $H_3C\cdots H_{ad}Pd$ distance, and verify that the ground state and excited states due to the excitation within Pd have energy minima around H_3C–H_{ad}=1.1 Å, while the charge transfer state in which the electron is transferred from CH_4 to Pd is repulsive, so the transition to this state causes the CH_{ad} bond dissociation. These results are similar to the CH_4–Pt case.

2. CH_4–Pd_7

In the Pd_7 cluster, six neighboring Pd atoms in the surface layer were included in addition to CH_4–Pd_{ad} (Pd_{ad} means Pd atom on which CH_4 adsorbs: see Fig. 1). We first carried out the RHF calculation for the Pd_7 cluster. At the RHF level, all seven Pd atoms have atomic populations close to d^{10}. Then, we selected one occupied d orbital composed mainly of Pd–$4d_{z^2}$ and three unoccupied orbitals composed mainly of Pd_{ad} $5s$, $5p_x$, and $5p_y$ atomic orbitals, respectively, as the active orbitals for the following SA-CASSCF calculation. Although $5p_x$ and $5p_y$ orbitals do not contribute to the interaction between CH_4 and Pd_7, it was difficult to exclude these orbitals from the active space since they are stabilized due to the interaction with neighboring Pd atoms. Of course, eight valence orbitals and the $3s$-Rydberg orbital of CH_4 were included in the active space. In total, the active space contains ten electrons and 13 orbitals. We carried out the SA-CASSCF calculation with this (10/13) active space for the CH_4–Pd_7 system. The ground state electronic structure is similar to the RHF results; Pd_{ad} has an atomic orbital population, $d^{9.9}s^{0.2}p^{0.2}$. The lowest charge transfer state ($CH_4\rightarrow Pd_7$ electron donation) lies 8.98 eV above the ground state. The atomic orbital population of Pd_{ad} in this charge transfer state is $d^{9.8}s^{0.5}p^{0.2}$ which is also close to d^{10}; d and p populations do not change significantly from the ground state, while the s population increases due to the electron donation from the CH_4 Rydberg orbital. The charge transfer state in which Pd_{ad} has an atomic population of d^9s^1 lies 0.44 eV above the lowest charge transfer state. On the other hand, in the CH_4–Pt_7 system,[7] the d^9s^1-like configuration of Pt_{ad} is more stabilized by the SA-CASSCF calculation. In addition, the atomic orbital population of Pt_{ad} in the charge transfer state is close to d^9s^1 rather than to d^{10} although the atomic populations of other six Pt atoms remain to be d^{10}-like in both Pt_7 and Pd_7 systems.

Next, we proceed to the calculation of the PEC with respect to the C–H_{ad} distance. The active space (10/13) just mentioned is too large to calculate the PEC, so it needs to be reduced. As mentioned above, Pd $5p_x$ and $5p_y$ do not contribute to the interaction between the excited state of CH_4 and the ground state of the Pd_7 cluster, but it turned out to be difficult to exclude these two orbitals which form a pair of e symmetry. Thus, for the calculation of the PEC, we excluded only the $5p_y$ orbital (a'' in C_s symmetry) from the (10/13) active space using a symmetry restriction, resulting in the (10/12) active space. Such a procedure breaks a degeneracy of e symmetry orbitals, but we found that the unbalanced treatment of e orbitals has only negligible effect on the calculated results, i.e., the excitation energy, the atomic orbital population, etc. Table II summarizes the leading electronic configurations, the excitation energy, and oscillator strength for the ground and several excited $^1A_1$ states for CH_4–Pd_7

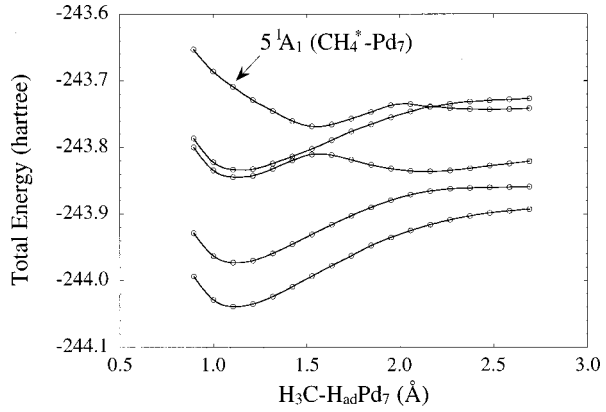

FIG. 2. Adiabatic potential energy curves of the ground and excited $^1A_1$ states for $H_3CH_{ad}Pd_7$ as a function of the C–H_{ad} distance calculated by the SA-CASSCF (10/12) method. Three lowest excited states correspond to the intracluster excitation, while the fifth state to the direct excitation. The H_{ad}–Pd_{ad} distance is fixed at 2.254 Å given in Table I.

calculated by the SA-CASSCF (10/12) method. We verified that the excitation energies and atomic orbital populations are not varied significantly by the reduction of the active space by comparing with the SA-CASSCF (10/13) results mentioned above. Three lowest excited states ($2^1A_1-4^1A_1$) are intracluster excited states, while 5^1A_1 is the charge transfer state. The dominant electronic configurations in this 5^1A_1 state indicates that this state originates from the direct excitation of CH_4 (the electron is excited from the CH_4 bonding orbital; see Table II). We encountered another problem on the calculation of PECs. As the C–H_{ad} bond length increases, the CH_{ad} bonding orbital is destabilized, and consequently, it mixes significantly with plural *d* orbitals of Pd_7. This means that one needs to take a larger active space than (10/12) or (10/13) to represent the excitation from the CH_{ad} bonding orbital, which requires a diagonalization of a very large matrix. To avoid this difficulty, we carried out the RHF calculation for CH_4 and Pd_7 separately, and merged two sets of orbitals to get one set of orbitals, which we used as reference orbitals for the SA-CASSCF calculation *without the RHF calculation for the entire* CH_4Pd_{10} *system*. The occupied *d* orbitals which have not been taken as active orbitals remain to be those determined by the RHF calculation for Pd_7. Such a procedure restricts the interaction between CH_4 and Pd_7 to be that between CH_4 and the active Pd_7 *d* orbital (and RHF unoccupied orbitals). We confirmed that such a reduction does not affect the calculated results at the equilibrium geometry (C–H_{ad} $=1.1$ Å).

Figure 2 shows the calculated PECs of the ground and several excited states with respect to the C–H_{ad} distance. The calculated PECs resemble qualitatively those obtained for the CH_4–Pt or CH_4–Pt_4 system in the previous study.[7] Three lowest excited states are due to the intracluster excitations, and have energy minima around C–$H_{ad}=1.1\,A$, while the fourth excited state is a charge transfer state in which the electron is donated to the Pd_7 cluster, leading to the dissociation of C–H_{ad}. Although the charge transfer state correlates to the ground states in the dissociation limit in both Pt and Pt_4 cases,[7] it does not in the Pd_7 cluster.

In the above calculations, atomic orbital populations of Pd_{ad} and other Pd atoms are close to d^{10} in both the ground and the charge transfer states, indicating that the *d* band of the Pd_7 cluster are filled completely. This is probably because an atomic character of Pd tails in the Pd_7 cluster. However, in the Pt_7 case, Pt_{ad} prefers the d^9s^1-like configuration to d^{10}, and, as we see later, the most stable configuration of Ni_{ad} in Ni_7 is also close to d^9s^1. Because energy band structures and density of states of Pt, Pd, and Ni crystals resemble each other, it is not realistic that the *d* band is filled completely only in the Pd surface. So, we obtained a reference wave function of Pd_7 by means of the restricted open-shell Hartree–Fock (ROHF) calculation in which d_{z^2} and *s* orbitals are singly occupied with the triplet spin multiplicity, and carried out the SA-CASSCF calculation for CH_4–Pd_7 with the specification of the singlet multiplicity. It is found that, when using the ROHF triplet orbitals as the reference orbitals for Pd_7, the ground state of CH_4–Pd_7 has the d^9s^1-like configuration for Pd_{ad}, and is stabilized by 12.6 kcal/mol in comparison with the one calculated using the reference orbitals obtained by the RHF calculation. In addition, the lowest charge transfer state, lying 8.40 eV above the ground state, also has the d^9s^1-like configuration for Pd_{ad}, which coincides with the CH_4–Pt_7 case.[7]

3. CH_4–Pd_{10}

In the RHF calculation for the Pd_{10} cluster, the atomic populations of the central Pd atom, six surrounding Pd atoms in the surface layer, and three Pd atoms in the second layer are $d^{10.05}s^{0.45}p^{0.5}$, $d^{9.75}s^{0.15}p^{0.1}$, and $d^{9.75}s^{0.25}p^{0.1}$, respectively, and the net charges are calculated as -0.84. 0.13, and 0.01 for the respective atoms. Note that smaller basis sets were used for nine surrounding Pd atoms in the surface and second layers. The negative charge of the central Pd atom is probably due to this unbalanced basis sets. We carried out SA-CASSCF (10/12) calculations for CH_4–Pd_{10} with the same active space as the CH_4–Pd_7 case. The frozen core orbitals were determined by RHF calculations not for the entire CH_4–Pd_{10} system, but for the respective CH_4 and Pd_{10}. In Pd_{10}, the atomic orbital populations of Pd atoms come to be indistinguishable among different states, as seen in the Pt_{10} system.[7] The charge transfer state lies 8.13 eV above the ground state, which is slightly more stable than the CH_4–Pd_7 case. In the ground state, the atomic orbital population of Pd_{ad} is $d^{9.7}s^{0.5}p^{0.6}$, while it is $d^{9.7}s^{0.6}p^{0.5}$ in the charge transfer state. Through a transition from the ground state to the charge transfer state, the charge is delocalized over the Pd_{10} cluster, which is reflected by the result that the atomic orbital population of Pd_{ad} does not change largely.

Figure 3 shows PECs for the CH_{ad} dissociation in CH_4–Pd_{10} calculated by the SA-CASSCF (10/12) method. There is no large differences compared with the CH_4–Pd_7 case (Fig. 2).

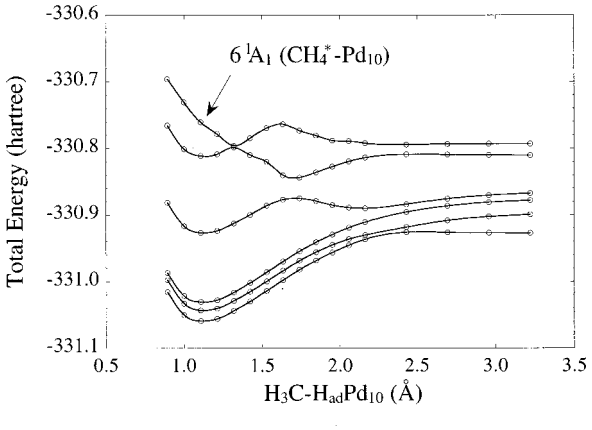

FIG. 3. Adiabatic potential energy curves of the ground and excited $^1A_1$ states for $H_3CH_{ad}Pd_{10}$ as a function of the C–H_{ad} distance calculated by the SA-CASSCF (10/12) method. Four lowest excited states correspond to the intracluster excitation, while the sixth state to the direct excitation. The H_{ad}–Pd_{ad} distance is fixed at 2.254 Å given in Table I.

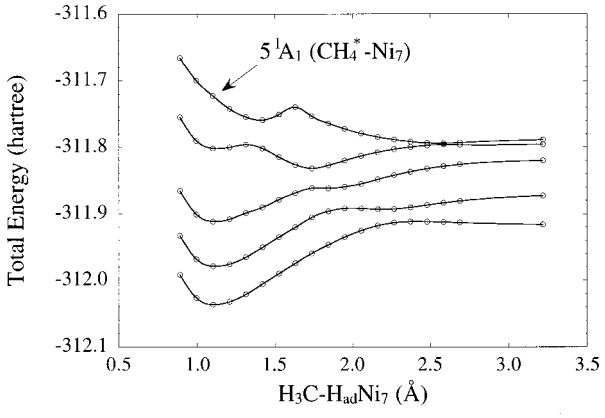

FIG. 4. Adiabatic potential energy curves of the ground and excited $^1A_1$ states for $H_3CH_{ad}Ni_7$ as a function of the C–H_{ad} distance calculated by the SA-CASSCF (10/12) method. Three lowest excited states correspond to the intracluster excitation, while the fifth state to the direct excitation. The H_{ad}–Ni_{ad} distance is fixed at 2.365 Å given in Table I.

C. Ni(111) surface

1. CH_4–Ni

So far, only one *d* orbital of a metal atom or cluster was included in the SA-CASSCF active space [(10/11) or (10/12)]. However, since Ni has the $3d^84s^2$ electronic configuration in the ground state (^3F), such a strategy seems not to be applicable to estimate the interaction between CH_4 and Ni. On the other hand, the inclusion of more than two *d* orbitals of Ni in the active space will require the large scale matrix diagonalizations and the state averaging. Taking into account that the degeneracy of *d* orbitals splits due to a crystal field by neighboring metal atoms, it is expected that neglecting such a near-degenerate effect should not be critical in comparison with the atomic system. Therefore, we carried out the SA-CASSCF calculation for CH_4–Ni with the same active spaces as those employed for CH_4–Pt and CH_4–Pd systems, in which four *d* orbitals of Ni are treated as the frozen core. Note that our object is not a reaction between CH_4 and the Ni atom, but a reaction between CH_4 and the Ni surface.

In the SA-CASSCF calculation for CH_4–Ni the charge transfer state lies 8.61 eV above the ground state, and Ni has the d^9s^1-like configuration in both the ground state and the charge transfer state. This result is close to the CH_4–Pt case in the previous study.[7]

2. CH_4–Ni_7

The SA-CASSCF calculations of PECs for the CH_{ad} dissociation in CH_4–Ni_7 were carried out in the same way as in the CH_4–Pt_7 and CH_4–Pd_7 systems; the orbitals for CH_4 and Ni_7 were determined by the RHF method, respectively, and two sets of RHF orbitals were merged to get one set of orbitals, which was used as reference orbitals for the SA-CASSCF calculation on the entire system. Figure 4 shows the calculated PECs with respect to the C–H_{ad} distance. The ground and excited states show qualitatively the same behavior as in the Pt_7 and Pd_7 cases: the ground state and the excited states due to intracluster excitations have energy minima around the equilibrium C–H_{ad} distance, while the charge transfer state in which the electron is donated from CH_4 to Ni_7 shows a repulsive profile, leading to the dissociation of CH_{ad}. Table III summarizes the leading electronic configurations for the ground state X^1A_1, the intracluster excited states 2^1A_1–4^1A_1, and the charge transfer state $5\ ^1A_1$, as well as the excitation energy and the oscillator strength for the respective excited states. The excitation energy to the charge transfer state was calculated as 8.53 eV. The atomic orbital population of Ni_{ad} is close to d^9s^1 in both the ground and charge transfer states, which coincides with the Pt_7 and Pd_7 (triplet) cases.

It must be noted that an energy barrier for the dissociation of CH_{ad} in the 4^1A_1 (intracluster excited) state is rather small, 3.52 kcal/mol, while the corresponding value in the Pt_7 case was calculated as about 14 kcal/mol. This difference can be understood by differences in the energy gradients of the charge transfer state at the equilibrium point. Figure 5 shows schematically this situation. According to the relations of the energy levels of the charge transfer state at the equilibrium structure and at the dissociation limit, one can see the larger energy gradient of the repulsive charge transfer state at the equilibrium point. Since the energy difference between the charge transfer state and the intracluster excited state at the equilibrium point in the Ni_7 case is almost the same as that in the Pt_7 case, the larger energy gradient should make the location of the avoided crossing point between the charge transfer state and the intracluster excited state closer to the equilibrium point in the Ni_7 case, resulting in the lower activation barrier. Such a small barrier in the 4^1A_1 state indicates the dissociation due to the surface-mediated excitation. However, as shown in Table III, the oscillator strength for the charge transfer state is larger than that for the intracluster excited state, so the intracluster excitation may be a minor process. Note that the other intracluster excited states, 2^1A_1 and 3^1A_1, show a bound feature in the energy profiles, and so are not leading to the CH_{ad} dissociation.

TABLE III. Leading configurations,[a] the excitation energy (eV), and the oscillator strength (a.u.) for ground and excited states of CH_4–Ni_7 calculated by the SA-CASSCF (10/12) method.

State[b]	Natural orbitals[c]				Coefficient	Excitation energy	Oscillator strength
	$CH-a_1$	$3d_{z^2}$	$4s-\sigma$	$4s-\sigma^*$			
X^1A_1	2	0	2	0	0.598	···	···
	2	2	0	0	−0.574		
	2	1	1	0	−0.469		
2^1A_1	2	0	2	0	0.709	1.56	6.98×10^{-4}
	2	1	1	0	0.633		
3^1A_1	2	0	1	1	0.843	3.41	2.78×10^{-1}
	2	1	0	1	0.437		
4^1A_1	2	2	0	0	0.667	6.39	8.41×10^{-3}
	2	1	1	0	−0.509		
	2	1	0	1	0.315		
5^1A_1	1	2	1	0	0.856	8.53	4.57×10^{-2}

[a]With an absolnte value larger than 0.3.
[b]2^1A_1, 3^1A_1, and 4^1A_1 correspond to an intracluster excited state; 5^1A_1 corresponds to the lowest charge transfer state.
[c]$3d_{z^2}$ denotes $Ni_7-3d_{z^2}$ orbitals; $4s-\sigma$ denotes the bonding orbital between Ni_7-4s and CH_4-3s; $4s-\sigma^*$ denotes the corresponding antibonding orbital.

3. CH_4–Ni_{10}

For the Ni_{10} cluster, we first carried out RHF calculations with employing two kinds of basis sets: the basis set of double-zeta quality $[2s2p2d]$ on Ni_{ad} and the smaller basis set $[2s1p1d]$ for nine surrounding Ni atoms (BS-1); $[2s2p2d]$ for seven Ni atoms on the surface layer and $[2s1p1d]$ for three Ni atoms on the second layer (BS-2). There are two kinds of $4s$-related orbitals in which all Ni–$4s$ orbitals overlap each other in the same signs ($4s_+$) or with one nodal plane between Ni_{ad} and a ''cage'' composed of the nine surrounding Ni atoms ($4s_-$). With the smaller basis set BS-1; $4s_+$ is occupied, and $4s_-$ is the lowest unoccupied $4s$-related orbital; the atomic orbital populations are d^{10} for Ni_{ad} and d^9s^1 for the other Ni atoms. On the other hand, with the basis set BS-2, $4s_+$ is the lowest unoccupied $4s$-related orbital, which is also valid for Ni_7 and for Pd_{10} calculated with BS-1. Taking into account that $4s_-$ can also overlap with the CH_4-3s Rydberg orbital due to their extension in space, and that the orbital energy of $4s_+$ with BS-2 is comparable to that of $4s_-$ with BS-1, we carried out the SA-CASSCF (10/12) calculation for CH_4–Ni_{10} by employing RHF orbitals obtained with BS-1, including $4s_-$ in the active space. However, the excitation energy of the charge transfer states was calculated as 10.17 eV (E state) and 10.64 eV (A_1 state), which implies no significant stabilization. This may be because of the nodal plane between Ni_{ad} and the Ni_9 ''cage'' in $4s_-$. Thus, we carried out the SA-CASSCF (10/12) calculation for CH_4–Ni_{10} by employing RHF orbitals obtained with BS-2. The excitation energy of the lowest charge transfer state was calculated as 8.76 eV. which is significantly stabilized relative to that of the isolated CH_4 molecule. Atomic populations of six surrounding Ni atoms on the surface layer can be expressed approximately as $d^{9.4}s^{0.5}$ in all the calculated states, which is interpreted as a mixture of two electronic configurations, d^9s^1 and d^{10}. On the other hand,. the atomic orbital populations of three atoms on the second layer, to which the small $[2s1p1d]$ basis sets were applied, are close to d^9s^1. The atomic population of Ni_{ad} in the ground and the charge transfer state is expressed

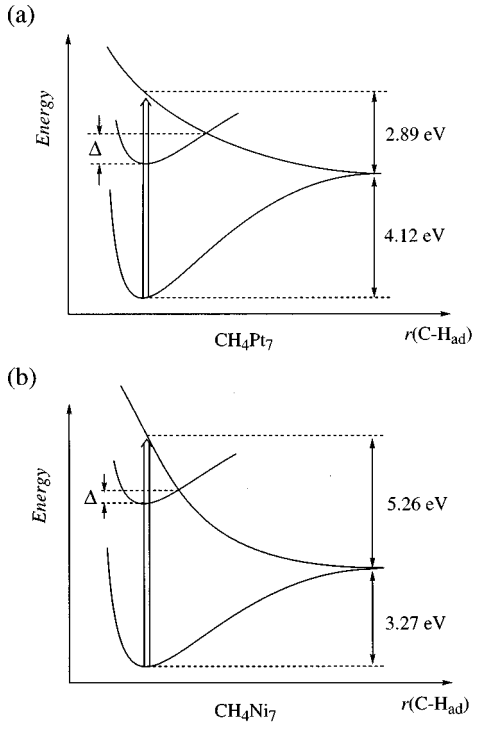

FIG. 5. Schematic illustrations of the difference of the energy barrier Δ for the C–H dissociation in the intracluster excited state of (a) CH_4–Pt_7 and (b) CH_4–Ni_7. In CH_4–Pt_7 there occurs an avoided crossing between the intracluster excited state and the charge transfer state far from the equilibrium CH_{ad} distance, resulting in a large energy barrier. In CH_4–Ni_7, the avoided crossing point is close to the equilibrium point because of the larger energy gradient of the charge transfer state, resulting in the smaller energy barrier for the C–H_{ad} dissociation.

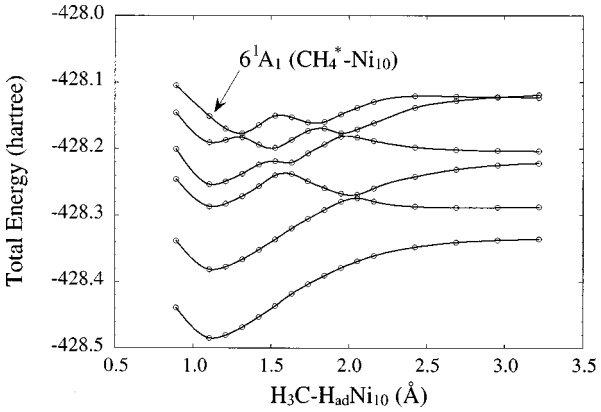

FIG. 6. Adiabatic potential energy curves of the ground and excited $^1A_1$ states for $H_3CH_{ad}Ni_{10}$ as a function of the C–H_{ad} distance calculated by the SA-CASSCF (8/10) method. Four lowest excited states correspond to the intracluster excitation, while the sixth state to the direct excitation. The H_{ad}–Ni_{ad} distance is fixed at 2.365 Å given in Table I.

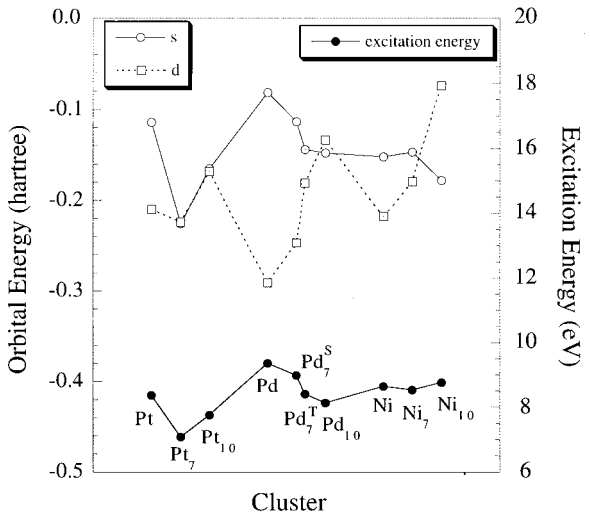

FIG. 7. Variations of energies of *d* and *s* (natural) orbitals of the central metal atom, and the excitation energy of the charge transfer state calculated for Pt, Pd, and Ni clusters. S and T in the superscript of Pd_7 indicates the spin multiplicity, singlet and triplet, respectively.

as $d^{9.3}s^{0.5}p^{0.5}$ and $d^{9.3}s^{0.9}p^{0.6}$, respectively, which implies that the electron is transferred to Ni $4s$ and $4p$ orbitals.

We calculated the PECs of the ground and excited states including the charge transfer state by means of the SA-CASSCF method with the basis set BS-2. The active space (10/12), employed for the other systems, requires considerable computational tasks for CH_4–Ni_{10}, so we tried to reduce the active space further. Since two degenerate bonding orbitals of CH_4, composed of carbon $2p_x$ and $2p_y$, should not participate in the dissociation process of CH_{ad}, it is expected that the exclusion of these two orbitals from the active space does not affect profiles of PECs for the dissociation. However, we failed to exclude both $2p_x$ and $2p_y$ orbitals from a technical reason, so only bonding and antibonding orbitals related to $2p_y$ of a'' in C_s symmetry were excluded from the (10/12) active space [resulting in the (8/10) active space], which causes the violation of the degeneracy. Note that it was verified that the violation of the degeneracy does not cause a fatal error in calculations for Pd_n and Ni_n clusters. Figure 6 shows the PECs for the CH_4 bond dissociation of CH_4–Ni_{10} calculated by the SA-CASSCF (8/10) method. There is no large difference in comparison with the PECs calculated for CH_4–Ni_7 or other systems already discussed.

D. Comparison among Pt, Pd, and Ni surfaces

Figure 7 shows variations of energies of *d* and *s* (natural) orbitals of the central metal atom, and the excitation energy of the charge transfer state calculated for Pt, Pd, and Ni clusters. It is readily seen that the excitation energy depends on the stability of the *s* orbital, and has no relation to energy levels of the *d* orbital, although these two orbitals often mix with each other due to the hybridization.

As to the PECs related to the CH dissociation, there is no large difference among the three metal surfaces. The charge transfer states show a repulsive energy profile along the CH dissociation, indicating that the C–H dissociation readily occurs. Although there are surface-mediated dissociation channels near the charge transfer states the oscillator strengths of these indirect excited states are calculated to be small compared to that of the charge transfer states. In conclusion, the direct excitations followed by the dissociations should be a major process on the Pt, Pd, and Ni(111) surfaces.

IV. CONCLUSIONS

In the present study, DFT and *ab initio* molecular orbital calculations were carried out to clarify the mechanisms of the initial excitation in the C–H photodissociation of CH_4 adsorbed on Pd and Ni(111) surfaces, as well as to verify the similarity and the difference from the reaction mechanism detected for the CH_4/Pt(111) system.[7] The adsorption site was assumed to be a onefold on-top site as employed for CH_4/Pt(111), and the adsorption geometries were determined by the B3LYP method. It is verified that CH_4 adsorbs on Pd and Ni surfaces weakly as on the Pt surface, which is in qualitative agreement with experiments. The electronic structure of the Rydberg state of CH_4 adsorbed on the Pd or Ni surface was calculated by the SA-CASSCF method. It is found that the Rydberg excited state of CH_4 is significantly stabilized as approaching to the metal surface, by growing into the charge transfer state in which the electron is donated from CH_4 to the substrate. We also discussed the relation between the stability of the charge transfer state and the electronic structure of the metal cluster. It proves that the stability of the charge transfer state depends on the energy level of the *s* orbital of the metal cluster. The PECs of the ground and excited states of CH_4–M_n (M=Pd, Ni; $n=7$, 10) were calculated as functions of the C–H_{ad} bond length, and it is found that the transition to the charge transfer state should lead to the C–H_{ad} bond dissociation on both Pd and Ni surfaces, coinciding with the results obtained for the Pt surface. Although there are several intracluster excited states near the charge transfer states, the oscillator strengths of these indirect excited states are calculated to be small compared to that of the charge transfer states. Therefore, it is expected that the

$C-H_{ad}$ dissociation should occur through the direct excitation (not through surface-mediated excitations) with a significant probability.

ACKNOWLEDGMENTS

The present research is supported in part by the grant-in-aid for scientific research from the Ministry of Education, Science and Culture of Japan. One of the authors (K.H.) also thanks the grant by Kawasaki Steel 21st Century Foundation.

[1] L. C. Lee and C. C. Chang, J. Chem. Phys. **78**, 688 (1983).
[2] G. Herzberg, *Electron Spectra and Electronic Structure of Polyatomic Molecules* (Van Nostland, New York, 1966), pp. 526–528.
[3] S. Karplus and R. Bersohn, J. Chem. Phys. **51**, 2040 (1969).
[4] M. S. Gordon and J. W. Caldwell, J. Chem. Phys. **70**, 5503 (1979).
[5] Y. Matsumoto, Y. A. Gruzdkov, K. Watanabe, and K. Sawabe, J. Chem. Phys. **105**, 4775 (1996) and references therein.
[6] X.-L. Zhou, X.-Y. Zhu, and J. M. White, Surf. Sci. Rep. **13**, 73 (1991).
[7] Y. Akinaga, T. Taketsugu, and K. Hirao, J. Chem. Phys. **107**, 415 (1997).
[8] F. C. Schouten, E. W. Kaleveld, and G. A. Bootsma, Surf. Sci. **63**, 460 (1977); F. C. Schouten, O. L. J. Gijzemann, and G. A. Bootsma, *ibid.* **87**, 1 (1979).
[9] J. R. Rostrup-Nielsen, in *Catalisys-Science*, edited by J. R. Anderson and M. Boudart (Springer, Berlin, 1984), Vol. 5.
[10] T. P. Beebe, Jr., D. W. Goodman, B. D. Kay, and J. T. Yates, Jr., J. Chem. Phys. **87**, 2305 (1987); L. Hanley, Z. Xu, and J. T. Yates, Jr., Surf. Sci. **L265**, 248 (1991).
[11] I. Chorkendorff, I. Alstrup, and S. Ullmann, Surf. Sci. **227**, 291 (1990).
[12] M. B. Lee, Q. Y. Yang, and S. T. Ceyer, J. Chem. Phys. **87**, 2724 (1987); S. T. Ceyer, J. D. Beckerle, M. B. Lee, S. L. Tang, Q. Y. Yang, and M. A. Hines, J. Vac. Sci. Technol. A **5**, 501 (1987); J. D. Beckerle, A. D. Johnson, Q. Y. Yang, and S. T. Ceyer, J. Chem. Phys. **91**, 5756 (1989); Q. Y. Yang, A. D. Johnson, K. L. Maynard, and S. T. Ceyer, J. Am. Chem. Soc. **111**, 8748 (1989); S. T. Ceyer, Science **249**, 133 (1990); S. T. Ceyer, Langmuir **6**, 82 (1990).
[13] A. V. Hamza and R. J. Madix, Surf. Sci. **179**, 25 (1987).
[14] H. Yang and J. L. Whitten, J. Chem. Phys. **96**, 5529 (1992).
[15] P. Kratzer, B. Hammer, and J. K. Nørskov, J. Chem. Phys. **105**, 5595 (1996).
[16] C. Lee, W. Yang, and R. G. Parr, Phys. Rev. B **37**, 785 (1988).
[17] A. D. Beeke, Phys. Rev. A **38**, 3098 (1988).
[18] B. Miechlich, A. Savin, H. Stoll, and H. Preuss, Chem. Phys. Lett. **157**, 200 (1989).
[19] See, for example, B. O. Roos, P. Bruna, S. D. Peyerimhoff, and R. Shepard, *Ab initio Quantum Chemistry II*, edited by K. P. Lawley [Adv. Chem. Phys. **67**, 63 (1987)].
[20] D. E. Woon and T. H. Dunning, Jr., J. Chem. Phys. **100**, 2975 (1989); *ibid.* **103**, 4572 (1995); T. H. Dunning, Jr., *ibid.* **90**, 1007 (1989).
[21] P. J. Hay and W. R. Wadt, J. Chem. Phys. **82**, 270 (1985).
[22] GAUSSIAN 94, Revision D.1, M. J. Frisch, G. W. Trucks, H. B. Schlegel, P. M. W. Gill, B. G. Johnson, M. A. Robb, J. R. Cheeseman, T. Keith, G. A. Petersson, J. A. Montgomery, K. Raghavachari, M. A. Al-Laham, V. G. Zakrzewski, J. V. Ortiz, J. B. Foresman, J. Cioslowski, B. B. Stefanov, A. Nanayakkara, M. Challacombe, C. Y. Peng, P. Y. Ayala, W. Chen, M. W. Wong, J. L. Andres, E. S. Replogle, R. Gomperts, R. L. Martin, D. J. Fox, J. S. Binkley, D. J. Defrees, J. Baker, J. P. Steward, M. Head-Gordon, C. Gonzalez, and J. A. Pople (Gaussian, Inc., Pittsburgh, PA, 1995).
[23] MOLPRO is a package of *ab initio* programs written by H.-J. Werner and P. J. Knowles, with contributions from J. Almlöf, R. D. Amos, M. J. O. Deggan, S. T. Elbert, C. Hampel, W. Meyer, K. Peterson, R. Pitzer, A. J. Stone, and P. R. Taylor. See also: H.-J. Werner and P. J. Knowles, J. Chem. Phys. **82**, 5053 (1985); P. J. Knowles and H.-J. Werner, Chem. Phys. Lett. **115**, 259 (1985); H.-J. Werner and W. Meyer, J. Chem. Phys. **73**, 2342 (1980); **74**, 5794 (1981); H.-J. Werner, Adv. Chem. Phys. **LXIX**, 1 (1987).
[24] K. Watanabe and Y. Matsumoto (private communication).